Effects of Silica Fume on Crack Sensitivity

Tests of high-performance concrete with varying silica fume contents show that no single parameter is sufficient for determining the risk of early-age cracking

BY T. KANSTAD, Ø. BJØNTEGAARD, E. J. SELLEVOLD, T. A. HAMMER, AND P. FIDJESTØL

To reap the benefits of impermeable high-performance concrete,* it is important to limit cracking. Experience has shown that concrete mixes with low water-cementitious materials ratios (*w/cm*) are particularly susceptible to early cracking if subject to conditions where deformations are restrained. However, evaluating concrete mixes in terms of sensitivity to early cracking is by no means simple. The sensitivity of concrete to cracking is a complex interaction between structural geometry and several material properties during the hardening process.

Our investigation was conducted to assess the crack sensitivity of high-performance concretes with different silica fume contents (0%, 5%, or 10%). First, we determined the material properties of these concretes, and then used this data to rate crack sensitivity by calculating the ratio of self-induced stress to strength over time under a variety of external conditions. We found that the effects of variations in silica fume content are of minor importance compared with other factors such as cement type, *w/cm*, structural configuration, degree of insulation, and environmental conditions.

Principles and procedures

Since the cracking risk in practice depends on the structural configuration of the concrete member and its relation to previously cast parts of the structure, this risk must be evaluated with a model that accounts for these external parameters. Using the model requires determination of the following material properties under isothermal and semiadiabatic conditions:

- Heat development;

* ***High-Performance Concrete*** (HPC) is concrete that meets special combinations of performance and uniformity requirements that cannot always be achieved routinely using conventional constituents and normal mixing, placing, and curing practices. Thus, a high-performance concrete is a concrete in which certain characteristics are developed for a particular application and environment. Examples of characteristics that may be considered critical in an application are: ease of placement, compaction without segregation, early age strength, long-term mechanical properties, permeability, density, heat of hydration, toughness, volume stability, and long life in severe environments. *(Editor)*

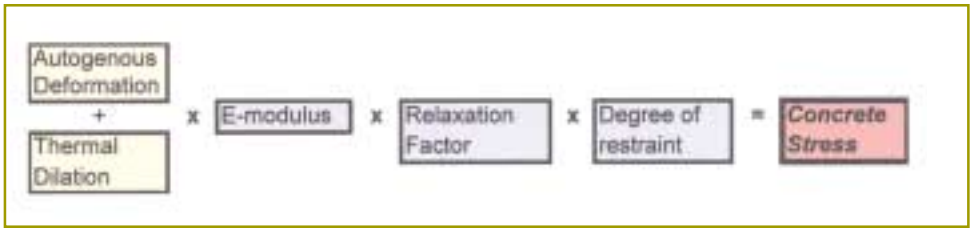

Fig. 1: Principle of stress calculation

- Coefficient of thermal dilation;
- Autogenous shrinkage;
- Mechanical properties (elastic modulus and tensile strength); and
- Relaxation behavior (deduced from uniaxial tests performed in a specially designed stress rig).

After partially verifying the model by running a simulation of the uniaxial loading condition established in the stress rig, we performed a time-step simulation of stress buildup using a finite-element model of the structure with the material parameters as input.

During hardening, thermal dilation and autogenous shrinkage occur simultaneously in the concrete mass, producing stress-generating deformations. Temperature changes due to heat of hydration and environmental conditions cause thermal dilation. Autogenous shrinkage is a result of continued hydration reactions in the cement, leading to self-desiccation (unlike drying shrinkage, which is due to water loss from the concrete). The amount of stress generated by thermal dilation and autogenous shrinkage in a given time interval depends on the degree of restraint of the concrete element, the elastic modulus, and the creep/relaxation properties of the concrete. The latter properties reduce a given stress increment over time.

Figure 1 illustrates the interplay of these factors, each of which changes with time. The stress at a given position at a given time is a consequence of the restraint conditions and the entire history of the concrete since setting. Thus, assessing risk of cracking at a given time and position involves comparing the calculated stress in the actual concrete structural element to the concrete tensile strength at the time.

Materials and concrete composition

The concretes tested[1-3] contained about 70% aggregate by volume and 0%, 5%, and 10% silica fume by weight of total binder. We also included some results for an equivalent concrete containing 15% silica fume.

The mixes had a *w/cm* of 0.40, a binder volume fraction of 28%, and 2 to 3% entrapped air. The amount of binder (cement and silica fume) was constant at 386 kg/m^3 (650 lb/yd^3); the amount of superplasticizer was adjusted to keep the slump for each concrete in the range of 160 to 180 mm (6.4 to 7.2 in.), which is common for bridge construction. All the concretes contained a low-alkali, high-strength cement, and all the aggregates were natural sand and gravel with a maximum diameter of 16 mm (0.64 in.). Approximately 3% of the aggregate passed the 0.125-mm (No. 120) sieve.

The mixes had the following 28-day compressive strengths:

- No silica fume = 75 MPa (10,900 psi);
- 5% silica fume = 80 MPa (11,600 psi); and
- 10% silica fume = 88 MPa (12,800 psi).

Experimental details

For each of the three concretes, we conducted numerous experiments to characterize the properties shown in Fig. 1. Also, adiabatic heat development measurements gave us a basis for calculating temperature development in the structures.

We measured tensile-strength and elastic-modulus development over time, under both isothermal (20 C [68 F]) and realistic temperature conditions (reaching 55 to 58 C [131 to 136 F] after 1 day and then gradually cooling to 20 C). An Instron test machine measured both properties on three parallel 100 x 100 x 600 mm (4 x 4 x 24 in.) specimens. Two linear variable differential transformers (LVDTs) mounted on the specimens measured deformation.

We also measured thermal dilation and autogenous shrinkage for the realistic temperature history and used the sum in the stress calculations, since there isn't a reliable model for separating the two effects. In an isothermal test, the thermal dilation is zero, and autogenous shrinkage is measured directly.

Creep/relaxation properties were not measured directly. However, for a slender concrete beam fully restrained against longitudinal movement and loaded in uniaxial tension, this is the only unknown property in stress calculations. A stress rig specially designed to conduct such a uniaxial test gave results that allowed us to check the validity of the creep/relaxation models used for the concretes (see "Stress Rig Tests" on p. 58).

Results

Heat development

Heat of hydration measurements showed that the silica fume had little effect. This is in line with earlier experience,[4] and implies that temperature development at a given position in a concrete structure depends largely on the initial concrete temperature, ambient conditions, dimensions of the structure, and degree of insulation, and not on silica fume dosage, as

long as the amount of cement and silica fume and the *w/cm* are constant.

Realistic temperatures

Figure 2 shows the realistic temperature developments imposed by the temperature control system on the concrete during the deformation and stress experiments. The differences between the temperature curves for the different mixes indicate the magnitude of the differences to be expected in a 600-mm (24-in.) thick wall. Testing mechanical properties under realistic temperatures followed a similar temperature history but with a somewhat lower maximum (55 to 58 C).

Tensile strength and elastic modulus

Figure 3 shows best-fit curves for the development of tensile strength and elastic modulus for the three test mixes. To permit comparison of data for tensile-strength and elastic-modulus development at different temperatures, we expressed the time scale as maturity (equivalent time at 20 C). This approach also simplifies the calculations.[1-3]

As Fig. 3(a) shows, increasing the silica fume dosage (S) increases tensile strength. The curves are based on a large number of data points—the majority from splitting-strength tests on 100 x 200 mm (4 x 8 in.) cylinders. Direct uniaxial tensile tests showed even greater positive effects of silica fume at high curing temperatures. Figure 3(b) shows that higher silica fume dosages also increase the elastic modulus. Though the increased tensile strength and the better performance at elevated temperatures with silica fume are beneficial in terms of cracking risk, the increased elastic modulus is detrimental, because a given restrained deformation (thermal dilation and autogenous shrinkage) will produce a higher stress.

Thermal dilation and autogenous shrinkage

We measured free strain in a special dilation rig[5] that allows free movement of a concrete specimen subjected to a controlled temperature history. Figure 4 shows pure autogenous shrinkage (at 20 C) from setting; in other words, only stress-inducing strains are plotted.[6] It can be seen that the autogenous shrinkage increases somewhat with silica fume dosage. However, most of the increase occurs during the first 2 days, when the elastic modulus is low, so it produces little stress.

Figure 5 shows thermal dilation and autogenous shrinkage (total strain) for a realistic temperature history (Fig. 2). The early expansion during heating is similar for all concretes, but the subsequent contraction caused by both cooling and autogenous shrinkage increases with silica fume dosage. In terms of stress buildup, this means more rapid buildup of tensile stresses with silica fume dosage (see "Stress Rig Tests" on p. 58)

We performed supplementary experiments to determine the thermal dilation coefficient.[5,7] In these experiments, the specimens underwent sudden temperature changes and we recorded the resulting strain. The ratio of strain to temperature change gives the thermal

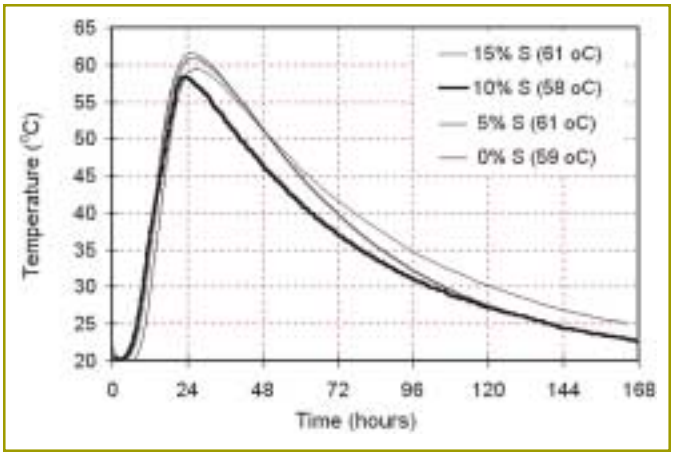

Fig. 2: Temperature histories imposed on the concrete in the deformation and stress experiments

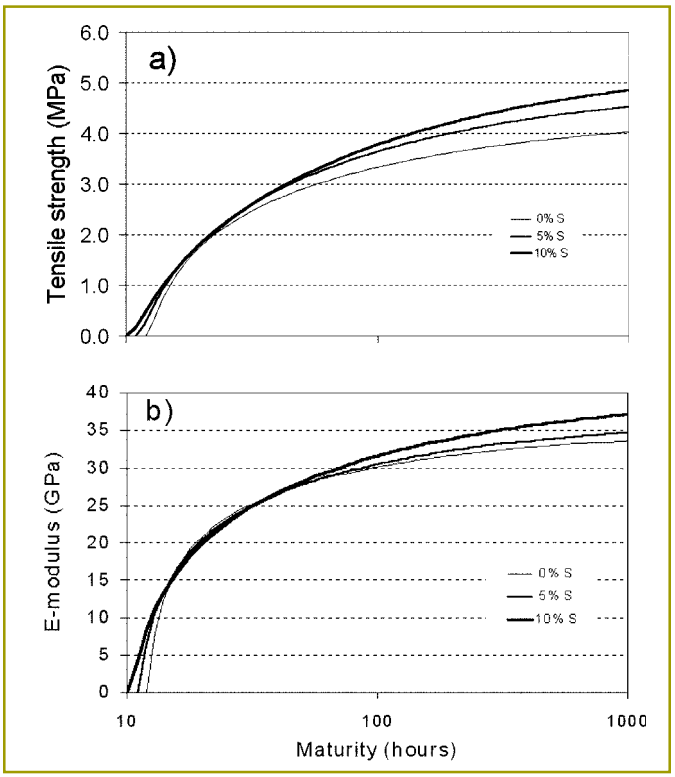

Fig. 3: Tensile strength (a) and elastic modulus (b) vs. maturity. (MPa = 145 psi, GPa = 145,000 psi)

dilation coefficient. Since the temperature history is known, it's then possible to calculate the thermal dilation component of the total strain in Fig. 5 and to subtract it from the total strain to produce the estimate for autogenous shrinkage, shown in Fig. 6. These results are interesting because during the first 2 to 3, days the autogenous shrinkage is very large for the silica fume mixes, but after this time, the autogenous shrinkage is small for all mixes and reverses to become expansion during the cooling period. Longer-term data[5] show that the expansion again reverses to contraction under 20 C

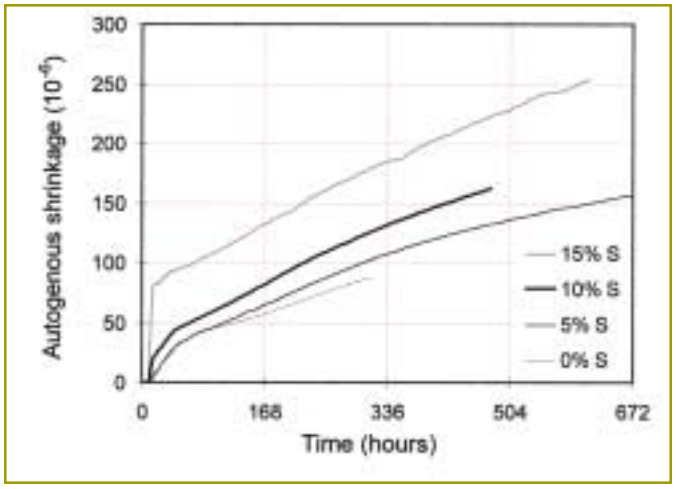

Fig. 4: Measured autogenous shrinkage at 20 C isothermal conditions

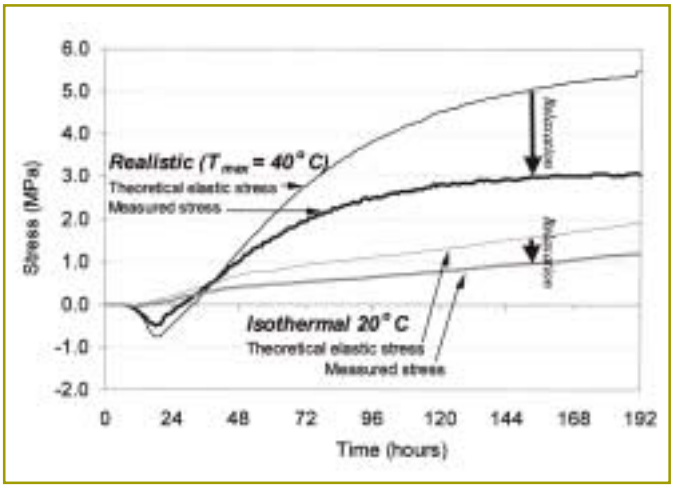

Fig. 7: Measured self-induced stresses under full restraint in the stress rig for concrete with 5% silica fume, compared to theoretical elastic stress curves calculated incrementally as free strain: (thermal dilation + autogenous shrinkage) × elastic modulus. Two temperature conditions: isothermal (20 C) and realistic (maximum temperature of 40 C) (MPa = 145 psi)

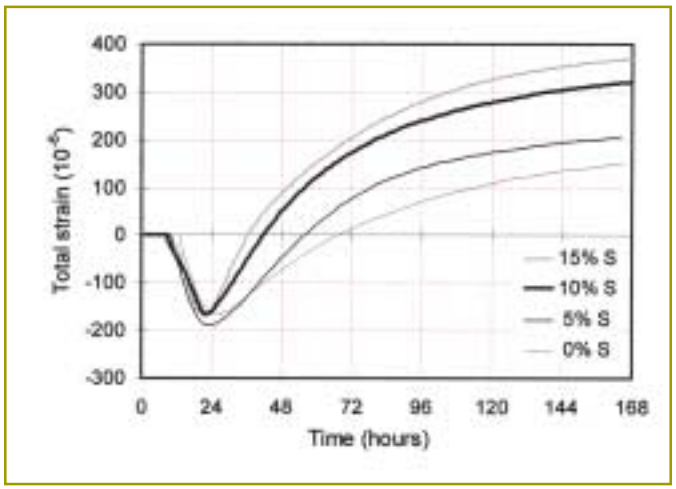

Fig. 5: Measured total strain, realistic temperature tests (T_{max} ≅ 60 C, see Fig. 2)

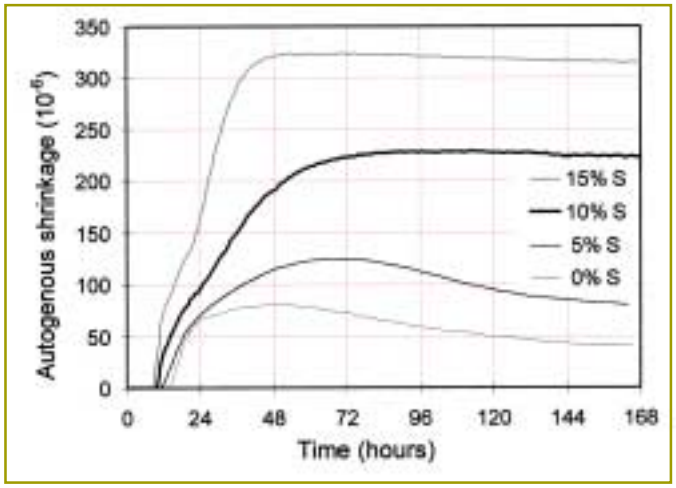

Fig. 6: Estimated autogenous shrinkage, realistic temperature tests (T_{max} ≅ 60 C, see Fig. 2)

isothermal conditions. Hence, isothermal measurements of autogenous shrinkage are very poor indicators of what may occur during realistic temperature histories.

Creep/relaxation

There is no simple way to illustrate the creep/relaxation behavior of concrete. For calculation purposes, we adjusted the parameters in the mathematical materials models to obtain a best fit with the stress rig results. Figure 7 shows the self-induced stresses measured under full restraint in the stress rig for concrete with 5% silica fume for two temperature histories: isothermal (20 C) and realistic (maximum temperature of 40 C [104 F]). We compared these stresses with theoretical elastic stress curves calculated incrementally as the product of free strain and the appropriate elastic modulus from Fig. 3. The arrows marked "relaxation" show the differences, or the reductions, in the elastically induced stresses caused by the viscoelastic nature of concrete. At 7 days, the reduction in stress is about 40% for both the realistic and isothermal temperature conditions. Thus, no major effect of temperature on relaxation is apparent in the 20 to 40 C range. For maximum temperatures above 40 C, however, further investigation is needed.[8]

Crack-risk simulations and conclusions

We used a culvert wall cast on an existing hardened base[9,10] to simulate our stress calculations. The formwork for the wall was removed after 4 days. In the simulation, we considered two values for maximum temperature inside the wall: low (30 to 33 C [86 to 91 F]) and high (47 to 51 C [117 to 124 F]). We also considered two types of cracking:

- Surface cracks caused by surface cooling and a hotter

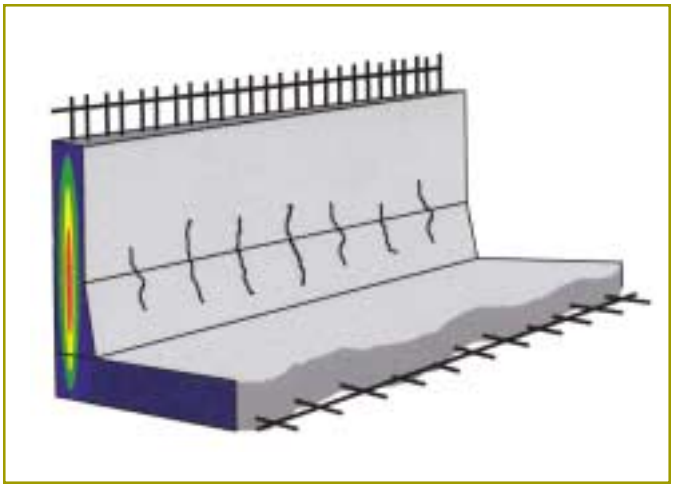

Fig. 8: Concrete structure used for the stress calculations

center, with the critical time for cracking at 4-1/2 days (1/2 day after form removal); and

- Through-cracks caused by external restraint from the hardened wall footing (critical time for cracking at 10 days). Figure 8 shows examples of through-cracks.

The crack-risk results are presented in Fig. 9 as ratios between calculated stresses (caused by thermal dilation and autogenous shrinkage) and tensile strengths (from Fig. 3). As expected, risk of cracking at the low-temperature range in the wall is always less than at the high range. The difference between "High 1" (using strength data from both uniaxial tensile tests and splitting tests) and "High 2" (using strength data from uniaxial tests only) is smaller for the silica fume concretes than for the reference. This indicates that the negative effect on tensile strength of a high curing temperature is larger for the reference concrete than for silica fume concrete.[1-3]

The results show that, in all cases, the total average risk of cracking is slightly smaller for the silica fume concretes than for the reference concrete. However, due to uncertainties involved in the assessments and procedures, it's more reasonable to conclude that all of the concretes have a similar risk of cracking. The risk of cracking for these three concretes is only marginally influenced by variations in composition (e.g., silica fume content) as long as the *w/cm* and the amounts of cementitious materials are kept constant. The primary factors determining cracking risk for these concretes include geometry, dimensions and restraints of the structure, and environmental factors (particularly temperature and form-removal time).

Based on this comprehensive analysis, no single concrete property (such as autogenous shrinkage) should be used to assess cracking risk; in practice, the interaction between several properties over time defines the risk. Presently this rigorous procedure, where no single parameter is sufficient, is considered necessary to evaluate the cracking risk of in-place concrete. With a larger amount of data available, it may be possible to eliminate some of the complex determination of material parameters by applying models based on material composition and ambient conditions.

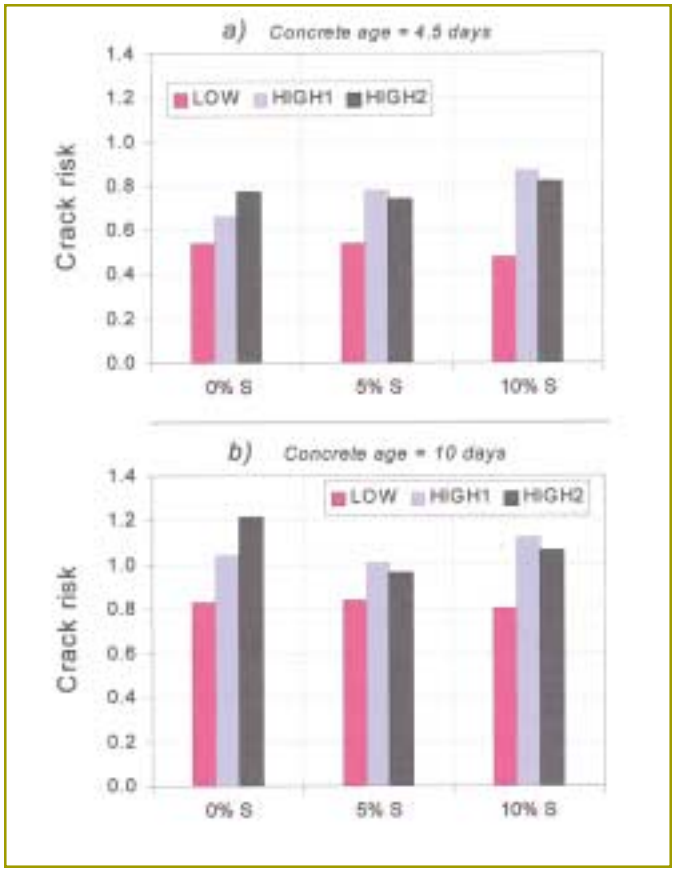

Fig. 9: Crack risk as a function of silica fume (S) dosage. Risk for surface cracks after 4.5 days (a) and risk for through-cracks after 10 days (b). LOW is for maximum wall temperature of 30 to 33 C; HIGH for 49 to 51 C. HIGH 1 uses all strength data, including splitting strength; HIGH 2 uses only uniaxial tensile-strength data

Acknowledgments

This paper is a product of the Brite-Euram Project IPACS (Contract BRPR-CT97-0437) and the associated Norwegian NOR-IPACS project. The financial contributions of the European Commission and the Norwegian Research Council are gratefully acknowledged.

IPACS partners are: Scancem AB (project leader), Selmer ASA, TU Delft, ENEL, TU Luleå, NCC AB, Skanska, Teknik AB, TU Braunschweig, Ismes, Norwegian Public Roads Directorate, Elkem ASA Materials, Norcem AS, and NTNU.

NOR-IPACS partners are: Selmer ASA (project leader), Elkem ASA Materials, Norcem A/S, Fesil ASA, Norwegian Public Roads Directorate, and NTNU.

References

1. Kanstad, T.; Bjøntegaard, Ø.; Sellevold, E. J.; and Hammer, T. A., *Crack Sensitivity of Bridge Concrete with Variable Silica Fume Contents*, NTNU Department of Structural Engineering, Trondheim, Norway, 2001.

2. Kanstad, T.; Hammer, T. A.; Bjøntegaard, Ø.; and Sellevold, E. J., "Mechanical Properties of Young Concrete: Part I–Experimental

Results Related to Test Methods and Temperature Effects," submitted for publication in *Materials and Structures*.

3. Kanstad, T.; Hammer, T. A.; Bjøntegaard, Ø.; and Sellevold, E. J., "Mechanical Properties of Young Concrete: Part II–Determination of Model Parameters and Test Programme Proposals," submitted for publication in *Materials and Structures*.

4. *Condensed Silica Fume in Concrete*, FIP state-of-the-art report, Thomas Telford, London, 1988.

5. Bjøntegaard, Ø., "Thermal Dilation and Autogenous Deformation as Driving Forces to Self-Induced Stresses in High-Performance Concrete," Doctoral thesis, NTNU Department of Structural Engineering, Dec. 1999, ISBN 82-7984-002-8.

6. Bjøntegaard, Ø.; Kanstad, T.; Sellevold, E. J.; and Hammer, T. A., "Stress-Inducing Deformations and Mechanical Properties of High-Performance Concrete at Very Early Ages," Fifth International Symposium on Utilization of High-Strength/High-Performance Concrete, Sandefjord, Norway, June 1999.

7. Bjøntegaard; Ø., and Sellevold, E. J., "Interaction between Thermal Dilation and Autogenous Deformation in High-Performance Concrete," *Materials and Structures*, V. 34, June 2001, pp. 266-272.

8. Atrushi, D.; Bjøntegaard, Ø.; Bosnjak, D.; Kanstad, T.; and Sellevold, E. J., "Creep Deformations Due to Self-Stresses in Hardening Concrete, Effect of Temperature," Sixth International Conference on Creep, Shrinkage and Durability Mechanics of Concrete and Other Quasi-Brittle Materials, M.I.T., Cambridge, Mass., August 2001.

9. Bosnjak, D., "Self-Induced Cracking Problems in Hardening Concrete Structures," Doctoral thesis, NTNU Department of Structural Engineering, Dec. 2000, ISBN 82-7984-151-2.

10. Bosnjak, D., and Kanstad, K., "Numerical Simulation of Temperature and Strain Development in the Maridal Culvert," *RILEM*

Stress rig tests

A sketch of the stress rig we used to check the validity of the creep/relaxation models is shown. A 100% restraint condition is provided by an electronic feedback system that gives signals to a high-precision screw. The signal is generated by any length change in a 700-mm (28-in.) central section of the beam, which has a cross section of 90 x 100 mm (3.6 x 4 in.). The length of the 700-mm central section is kept constant via the screw that moves one of the anchoring heads of the specimen. At the other head, a load cell records the restraining force. A surrounding steel frame gives support and takes care of the counterforce. The specimen and the anchoring heads are in close contact with water tubes and are well-insulated externally. Temperature control is provided by circulating water in the tubes from a central bath.

The graph shows stress rig results for the 0%, 5%, and 10% silica fume test specimens performed under realistic temperatures and uniaxial full restraint, as well as results under partial restraint for concrete with 15% silica fume. Under partial restraint, the active deformation control of the stress rig is turned off, and only the steel frame of the rig provides restraint against deformations.

At full restraint, increases in silica fume dosage lead to increased self-induced stress in the period after 24 hours due to high autogenous shrinkage, and all three specimens fail at a tensile stress of about 3 MPa (435 psi). This corresponds well with the results in Fig. 6, which shows autogenous shrinkage increasing with silica fume dosage in the critical period beyond 24 hours, when the cooling rate also is high. In concrete structures, however, the degree of restraint is considerably less than 100% and, as demonstrated by the 15% silica fume concrete, the stress buildup will be much slower, particularly beyond the first 48 hours, when autogenous shrinkage contributes little or nothing to tensile stress. Such partial-restraint experiments record both stress buildup and deformations. The resulting curves are the basis for verification of the creep/relaxation models.

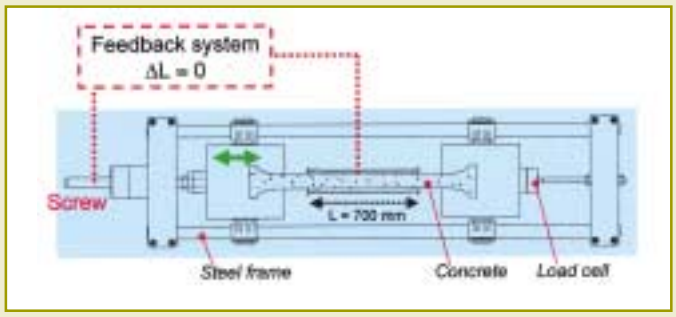

Sketch of the stress rig

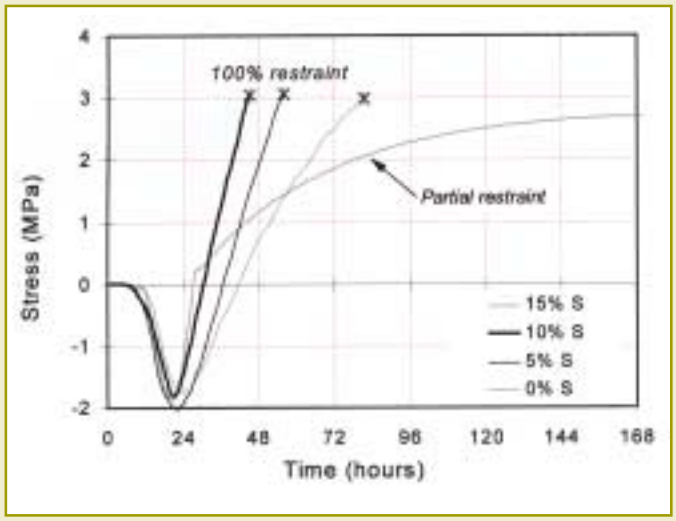

Stress development, realistic temperature tests (T_{max} ≅ 60 C, see Fig. 2) (MPa = 145 psi).

International Conference on Early Age Cracking in Cementitious Systems, K. Kovler and A. Bentur, eds., Haifa, Israel, March 2001.

Received and reviewed under Institute publication policies.

Terje Kanstad is an associate professor in the Department of Structural Engineering at the Norwegian University of Science and Technology (NTNU) in Trondheim, Norway. His work focuses on design rules for concrete structures, finite-element analysis, materials modeling, and time- and temperature-dependent behavior of young and hardened concrete.

Øyvind Bjøntegaard received his PhD from the Department of Structural Engineering at NTNU, where his main topic of study was the driving forces of self-induced stress generation in young concrete: autogenous shrinkage and thermal dilation. Since 1999, he has done postdoctoral research on stress generation in young concrete.

Erik J. Sellevold is professor of concrete technology at the Department of Structural Engineering at NTNU. Since receiving his PhD from Stanford University, he has worked at the Denmark Technological University, Norwegian Building Research Institute, Elkem Materials, and for the last 12 years at NTNU.

Tor Arne Hammer is a senior research engineer at SINTEF Civil and Environmental Engineering, Cement and Concrete. He received his MS degree from NTNU. His field of research is material properties of fresh and hardened concrete, including high-performance concrete and lightweight aggregate concrete.

FACI Per Fidjestøl is a graduate of NTNU. He is a senior specialist with Elkem ASA Materials and has worked in concrete technology for 25 years, mainly with high-performance concrete and silica fume. He is currently a member of the ACI Board of Direction, and he chairs ACI Committee 234, Silica Fume, in addition to membership in several other ACI committees.